

Energy Transfer in LH2 of *Rhodospirillum Molischianum*, Studied by Subpicosecond Spectroscopy and Configuration Interaction Exciton Calculations

Janne A. Ihalainen,^{*,†} Juha Linnanto,[†] Pasi Myllyperkiö,[†] Ivo H. M. van Stokkum,[‡] Beate Ücker,[§] Hugo Scheer,[§] and Jouko E. I. Korppi-Tommola[†]

Department of Chemistry, University of Jyväskylä, P.O. Box 35, FIN-40351 Jyväskylä, Finland, Division of Physics and Astronomy of the Faculty of Sciences, Vrije Universiteit, De Boelelaan 1081, 1081 HV Amsterdam, The Netherlands, and Botanisches Institut der Universität München, Menzinger Strasse 67, D-80638 München, Germany

Received: March 9, 2001; In Final Form: July 20, 2001

Two color transient absorption measurements were performed on a LH2 complex from *Rhodospirillum molischianum* by using several excitation wavelengths (790, 800, 810, and 830 nm) and probing in the spectral region from 790 to 870 nm at room temperature. The observed energy transfer time of ~ 1.0 ps from B800 to B850 at room temperature is longer than the corresponding rates in *Rhodopseudomonas acidophila* and *Rhodobacter sphaeroides*. We observed variations (0.9–1.2 ps) of B800–850 energy transfer times at different B800 excitation wavelengths, the fastest time (0.9 ps) was obtained with 800 nm excitation. At 830 nm excitation the energy transfer to the B850 ring takes place within 0.5 ps. The measured kinetics, as well as steady-state absorption and CD spectra, are consistent with those calculated with the configuration interaction exciton method (CIEM) [Linnanto et al. *J. Phys. Chem. B* 1999, 103, 8739]. Fully excitonic simulation of the CD spectrum of the LH2 of *Rs. molischianum* is presented for the first time. The calculations put the E_3 exciton states of B850 near the narrow excitonic B800 manifold and according to our model, these states provide the main route of energy transfer from the B800 ring to the B850 ring in the complex. The $1,2E_2$ states at 824 nm predicted by the calculations serve as an additional energy transfer channel as indicated by the observed fast transfer rate at 830 nm excitation.

Introduction

In phototropic organisms, nearly all energy for photosynthetic reactions is captured by light-harvesting complexes. Purple photosynthetic bacteria have two light harvesting complexes, LH1 and LH2, that absorb light and transfer excitation energy to the reaction center (RC). In the RC the excitation energy is used for a sequence of electron-transfer reactions, which creates a stable transmembrane charge separation.^{1,2}

LH2, LH1, and RC are well-organized assemblies of bacteriochlorophylls (BChl) and carotenoids. Each light harvesting complex contains a characteristic number of pigments at precise arrangement and orientation. The LH2 complex from *Rhodospirillum (Rs.) molischianum* has 24 BChl *a* molecules and at least eight carotenoids, most likely lycopenes.³ The basic unit of LH2 is an $\alpha\beta$ -heterodimer consisting of two protein subunits, often referred to as α - and β -apoproteins, which bind in total three BChl *a* molecules and at least one lycopene molecule. Eight $\alpha\beta$ -subunits are arranged in a circle and they form two BChl *a* rings. The first ring (B800) has eight BChl *a* molecules absorbing at 800 nm. The second ring (B850) has 16 BChl *a* molecules absorbing at 850 nm. A similar ring-shaped arrangement is characteristic of LH2 from *Rhodopseudomonas (Rps.) acidophila*, which consists of nine $\alpha\beta$ -subunits. The pigment orientation with respect to the symmetry axis is different from

that in LH2 of *Rs. molischianum*.⁴ The Mg–Mg distance between B850 BChls in LH2 of *Rs. molischianum* is 9.2 Å within the $\alpha\beta$ -heterodimer and 8.9 Å between the heterodimers. In the B800 ring the BChl Mg–Mg distance is 22 Å. The Q_y transition dipole moment of the B800 BChl *a* is nearly parallel to the respective transition dipole moment of the B850 BChl *a* in the same subunit, and to the membrane plane.³ This orientation of the Q_y transition dipole has been estimated from linear dichroism spectra.⁵ The pigment binding environment of the B850 aggregate is nonpolar while that of B800 is polar.³ Carotenoids are in close contact with BChl *a* molecules. Carotenoids absorb light in a spectral region complementary to that of BChls (around 500 nm), and they transport the light energy to BChls. The carotenoids act also as photoprotective agents, quenching the BChl excited triplet state.⁶

The energy transfer processes in LH2, such as from carotenoids to B800 or to B850 BChls and from B800 to B850 BChls, occur in the subpicosecond time scale. The excitation energy equilibrates very fast, in about 100 fs,⁷ among B850 pigments from where it is transferred to LH1 in a few picoseconds. The last energy transfer step in the PSU of purple bacteria is from LH1 to the RC and takes tens of picoseconds.⁶

Absorption at 800 nm is attributed to individual BChl *a* molecules of the B800 ring, whereas the B850 pigments form a strongly coupled excitonic system.⁶ This has been demonstrated, for example, by means of single molecule spectroscopy of B800–850 in *Rhodobacter (Rb.) sphaeroides* and by nonlinear techniques for several similar complexes.^{8,9} In various one-color pump–probe studies at 800 nm for LH2 complexes of purple bacteria, the fast ~ 400 fs component is observed and

* Corresponding author. E-mail: janihal@cc.jyu.fi. Fax: +358 14 2602551.

[†] University of Jyväskylä.

[‡] Vrije Universiteit.

[§] Universität München.

assigned as an intraband energy transfer process of B800.^{10–12} On the other hand, hole burning, fluorescence line narrowing, and three photon echo studies suggest that no 400 fs intraband (B800–B800) energy transfer takes place and only vibrational relaxation processes are observed.^{13–16} Reported anisotropy decay time constants, which yield information on energy transfer processes between differently oriented isoenergetic pigments, range from 0.4 to 1.2 ps.^{11,14,16–18} On the basis of anisotropy results Pullerits et al. have suggested that the intra-ring energy transfer follows the Förster mechanism.^{11,14} Additionally, Salverda et al. observed a very fast component (<100 fs), which was assigned to relaxation involving coupling of pigments to protein phonons.¹⁸ Noteworthy is that Lin et al. have reported that vibrational relaxation takes place in 0.5–1.0 ps in the RC from *Rb. sphaeroides*.¹⁹

The energy transfer from B800 to B850 is one of the most thoroughly studied energy transfer steps of light harvesting reactions.⁶ Transient absorption measurements give time constants of 0.7–0.8 ps for B800–B850 energy transfer in LH2 of *Rps. acidophila* and *Rb. sphaeroides*.^{11,15–17,20} The transfer time slightly increases upon lowering temperature.^{11,17} To our knowledge, room-temperature energy transfer rates in LH2 complex of *Rs. molischianum* have not been published. Wendling et al. have reported a B800–B850 energy transfer time of 1.7 ps for LH2 of *Rs. molischianum* at 77 K, by using one-color pump–probe experiments, and Wu et al. measured 1.9 ps at 4 K, by means of hole burning spectroscopy.^{12,21} Recently, the dependence of the B800–B850 energy transfer time on the energy gap between the B800 and B850 aggregates has been studied by exchanging of the BChls with different (B)Chl derivatives.^{22,23} As the B800 band shifts to the blue, the spectral overlap between the B800 and B850 Q_y bands decreases and the rate of energy transfer decreases; the measured time constants range from 0.9 ps (with BChl *a* in the B800 sites) to 8.3 ps (Chl *a* in the B800 sites).²³

The energy transfer mechanisms within and between B800 and B850 has been under debate since the first time-resolved spectroscopic results were published. In most cases the energy transfer mechanism has been considered as a Förster hopping mechanism.²⁴ The rate constants obtained from the “traditional” excitation hopping model with dipole–dipole interaction approximation are at least 5 times slower than the experimental B800–B850 energy transfer rates.^{11,23} If the electronic couplings are calculated in more detail, and other effects (electron–phonon coupling, site energy disorder, etc.) are considered, faster rates are obtained. The calculations of Scholes and Fleming focused on *Rb. sphaeroides*, and the electronic couplings were determined by using ab initio quantum chemical methods and the atomic coordinates of LH2 of *Rbs. acidophila*. Energy transfer was assumed to occur from a single B800 chromophore to the excitonic B850 aggregate.²⁵ However, the calculated rate constants, with dielectric screening not included, were still about a factor of 2 longer than the experimental rates. This discrepancy was attributed to the role of carotenoids in energy transfer. Krueger et al. reported a substantial mixing of the carotenoid and B850 orbitals, which may have a large influence on the B800–B850 coupling and therefore on the energy transfer rate.²⁶ Recently, new methods for calculating excitation energy transfer have been developed.^{27,28} It has been suggested that the energy transfer from B800 to higher optically forbidden states of B850 could be the dominant mechanism of the rapid excitation transfer.^{29,30}

In this article we present both experimentally determined and calculated B800–B850 energy transfer rates of the LH2

complex from *Rs. molischianum*. The measured values are determined by means of the two-color pump–probe technique at room temperature, with excitation wavelengths of 790, 800, 810, and 830 nm. The experimentally determined energy transfer times are compared with calculated constants, which were obtained by determining the excitonic energy levels of the donor and acceptor chromophore assemblies by using the CIEM method.³⁰ To obtain rate constants, Fermi’s Golden rule, experimental homogeneous and inhomogeneous line widths and coupling parameters that reproduce the absorption and CD spectra were used.²⁸

Materials and Methods

Sample Preparation. LH2 antenna complexes were isolated from *Rs. molischianum* DSM 119 as described in ref 22, and the isolated LH2 complexes were diluted in 20 mM Tris/HCl (pH 8.0) and 0.1% LDAO. The optical density (OD) at 850 nm of the sample was for the absorption and CD measurements around 0.7 cm⁻¹, for fluorescence below 0.1 cm⁻¹, and for the time-resolved measurements ~0.5 mm⁻¹.

Spectroscopy. The electronic absorption spectra were measured on a Perkin-Elmer Lambda 5 UV/vis spectrometer and the circular dichroism (CD) spectra were measured on a JASCO J-715 spectropolarimeter (optical path length of 1 cm for both measurements). Fluorescence emission spectra were measured with a 0.3 m imaging spectrograph (Acton Research Corporation) and a CCD camera (Princeton Instruments). The spectral resolution was 1 nm. For broadband excitation a tungsten halogen lamp (Oriel) was used with a band-pass filter transmitting at 455 nm (bandwidth of 20 nm). The spectra were recorded at room temperature.

Time-resolved absorption spectra were recorded by means of the two-color pump–probe technique. The excitation light was taken from a mode-locked Ti:sapphire laser (Coherent, MIRA 900, 76 MHz,) pumped with a solid-state diode-pumped frequency-doubled Nd:YVO₄ laser (Verdi-5W, Coherent) with a wavelength of 532 nm. Pulses were amplified with a regenerative Ti:sapphire amplifier pumped by a second harmonic Q-switched Nd:YLF laser (Quantronix). The repetition rate of the system was 1 kHz. The instrument response function was measured in CS₂ by using the optical Kerr effect. Excitation pulses were centered at 790, 800, 810, or 830 nm (fwhm ~6 nm) with intensities of ~36 nJ/pulse. The probe wavelengths covered a spectral region of 790–870 nm, at 5–10 nm intervals. The probe and reference pulses were taken from a white light continuum generated by focusing a part of the laser beam into a 2 mm sapphire plate. The intensity of each pulse (excitation, probe, and reference) was measured by using three photodiodes and a home-built data acquisition system. The white light of the probe and reference beams was spectrally resolved after the sample by using a home-built monochromator. The relative polarization of the pump and probe pulses was set to the magic angle (54.7°), except for the anisotropy measurements where parallel and perpendicular polarizations were detected.

Data Analysis. The analysis of the transient absorption data was done by using global analysis.³¹ An irreversible unbranched sequential two-step model, which provides (B800 $\xrightarrow{k_1}$ B850 $\xrightarrow{k_2}$) species associated difference spectra (SADS) and the time constants of the process(es), was used. The rate constant k_1 represents the energy transfer rate from B800 to B850, and k_2 is the reciprocal of the lifetime of B850. The instrument response function was modeled as a Gaussian function with fwhm of ~275 fs. A similar model has been used previously for LH2 of

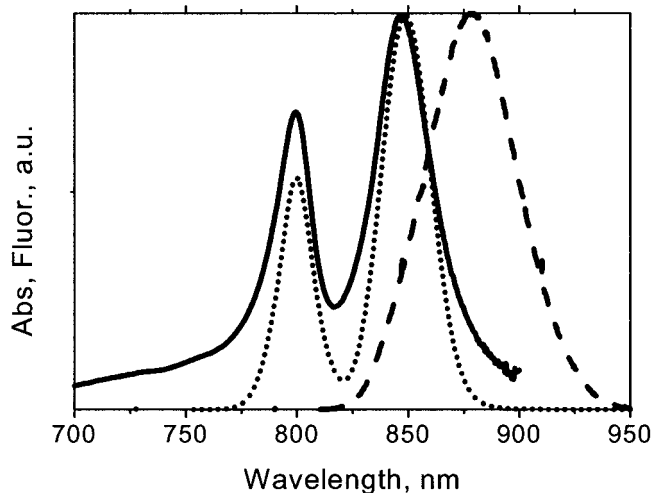


Figure 1. Absorption (solid) and fluorescence (dashed) spectra of LH2 from *Rs. molischianum* at room temperature. The calculated absorption spectrum is shown as a dotted line; see more details in text.

Rs. molischianum with the B800(blue) \rightarrow B800(red) energy transfer process included.¹²

Simulations. The absorption and CD spectra were calculated by using the same method that was previously used to calculate absorption and CD spectra of the LH2 complex of *Rps. acidophila*.³⁰ Briefly, the method combines a semiempirical configuration interaction calculation of electronic transitions of the monomeric and dimeric BChl's in the protein environment and exciton theory to obtain electronic energies and eigenstates of the aggregated chromophores. Both B800 and B850 rings are considered as excitonic assemblies. A statistical simulation accounting for the inhomogeneous line widths was used to calculate absorption and CD spectra of antenna complexes.

The structure of LH2 from *Rs. molischianum* was taken from the Brookhaven data bank [Brookhaven Protein Data Bank, ID code 1LGH], determined by Koepke et al.³ Homogeneous line widths were estimated at 188 and 200 cm^{-1} for the spectral regions of 870–815 nm and 815–600 nm, respectively. The homogeneous line width was assumed to have a Lorentzian line shape. The inhomogeneous broadening was accounted for by random Gaussian variation of the diagonal elements of the exciton matrix by 200 cm^{-1} for B800 and 220 cm^{-1} for B850 and by variation of the off-diagonal matrix elements by 10% of their value. The Q_y transition energies of monomeric pigments in their local protein environments were estimated by using semiempirical configuration interaction ZINDO/S CIS method. All amino acids with a distance of 7 Å from B850 BChl *a* and nine nearest amino acids from B800 BChl *a* were taken in the ZINDO/S CIS calculation with heavy atom coordinates fixed to structural data. The calculated site energy values corresponded to 768 and 763 nm for the two monomeric BChl *a*'s of B850 experiencing different local environments. For BChl *a* of B800 the site energy became 798 nm, which is very close to the experimental value (Figure 1) and almost the same as the site energy of the LH2 complex of *Rps. acidophila*.³⁰ Calculated site energies were used as diagonal elements of the exciton Hamiltonian. The value of the transition dipole moment of 6.13 D for monomeric BChl *a* was used. The dielectric constant of the protein matrix was taken as 2.1. The calculated nearest neighbor interaction energies in the B850 ring were 756 and 570 cm^{-1} . These interaction energies fit in with other theoretically predicted values for LH2 from *Rs. Molischianum*. Similar or higher values are reported in refs 32 and 33; lower values

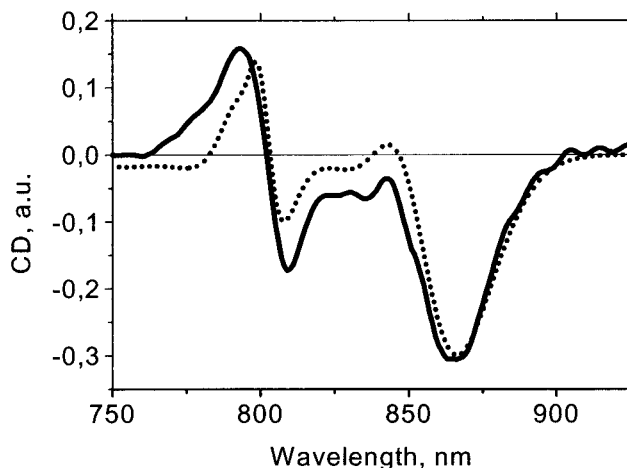


Figure 2. Experimental (solid) and calculated (dotted) CD spectrum of B800 and B850 bands of LH2 from *Rs. molischianum* at room temperature.

are reported in refs 34 and 35. However, none of these studies shows calculated steady-state spectra.

Calculations of B800 \rightarrow B850 excitation energy transfer rates were based on the use of excitonic energy levels, which produced the experimental spectra correctly and the Fermi's Golden Rule.²⁸ In energy transfer rate calculations some 5000 diagonalization cycles were carried out to account for inhomogeneous broadening. Homogeneous line widths were used as experimental input. Interested readers are advised to look at ref 30 for details of simulating the absorption and CD spectra and ref 28 for calculating the energy transfer rates. A detailed description of excitation motion in the B800 ring together with excitation energy transfer (EET) and their combined influence on the polarization changes in light harvesting complexes is an ongoing theoretical effort and results will be published elsewhere.³⁶

Results

Absorption Spectrum. Figure 1 shows the Q_y absorption (solid line) and fluorescence (dashed line) spectra of the purified LH2 complex at room temperature. In this region two absorption bands are observed one at 800 nm (B800) and one at 847 nm (B850). The calculated absorption spectrum is shown as a dotted line. The fluorescence maximum is located at 879 nm, originating most likely from the lowest excitonic energy level of the B850 system (1A state at around 870 nm, Figure 3). The spectra of LH2 B800–850 complexes of other purple bacteria are quite similar to the LH2 spectrum of *Rs. molischianum* with the exception that the B850 band of the latter is a few nanometers blue shifted as compared to the B850 band of the other species.^{15,16,22} The simulations suggest that this shift is due to pigment–protein interaction. Including only pigment–pigment interactions in the calculations gives *Rs. molischianum* the LH2 B850 band that is red shifted with respect to the corresponding band of *Rps. acidophila*. According to our calculations the protein environment changes the Q_y transition dipole in *Rs. molischianum* and the absorption maximum shifts toward blue, more than in *Rps. acidophila* (data not shown). This interaction affects also the CD spectrum of the complex (see below).

CD Spectrum. Figure 2 shows the room-temperature CD spectrum of our LH2 preparation. The measured spectrum is drawn as a solid line and the calculated spectrum as a dotted line. The spectrum consists of a conservative peak around 800

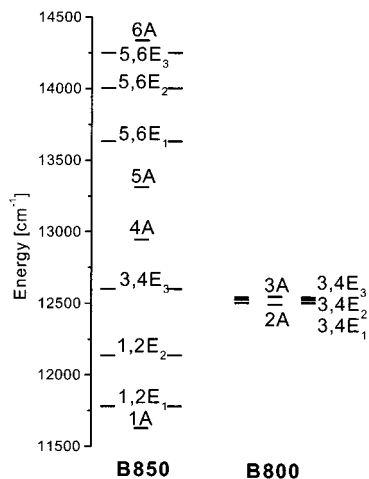


Figure 3. Calculated excitonic energy levels of LH2 of *Rs. molischianum*. On the left-hand side levels of the B850 ring and on the right-hand side levels of the B800 ring of the LH2 complex. The splitting of the B800 manifold is due to weak excitonic interaction.

nm and a nonconservative peak around 850 nm. A positive peak is located at 793 nm and shoulders at 777 and 798 nm whereas the negative peaks are located at 809 and 865 nm with shoulders at 836 and 891 nm. The LH1-like character of the amino acid sequence of LH2 of *Rs. molischianum* is reflected in the circular dichroism signal of the B850 band of this complex.⁵ A broad negative band around 780 nm in the CD spectrum of a B800-less mutated LH2 from *Rb. sphaeroides* has been observed and assigned to the upper excitonic state of the B850 ring.^{37,38} A similar transition can also be seen in our CD spectrum as a positive signal around 777 nm. Noteworthy is that this level is also present in the calculated energy level scheme (4A state of Figure 3).

The similarity between calculated and experimental absorption and CD spectra justifies the assumption that the energy level scheme, shown in Figure 3, describes the excitonic energies of the B800–850 complex of *Rs. molischianum*. The E_1 states have the most oscillator strength in both rings. The rotational strength is accumulated on the A and E_1 states. We want to point out that this is the first time that the CD spectrum of the LH2 from *Rs. molischianum* has been explained by using a fully excitonic model. The same set of parameters, which were used to calculate the absorption and CD spectra, were used for calculation of energy transfer rates among B800 pigments and between the B800 and B850 excitonic systems.

Transient Absorption Spectra. It has been proposed that the intensity of the pump pulse is a crucial parameter for observing real energy transfer processes in light harvesting antenna.^{10,16} High excitation intensity may lead to singlet–singlet annihilation due to rapid bimolecular quenching of excitons within the B800, and subsequent fast excitonic relaxation via the excitonic manifold of the B850 ring. Annihilation appears, if present, as exceedingly fast intensity dependent recovery of the ground-state bleach of the B800 band and as depletion of long-lived excited-state absorption below 840 nm.¹⁶ Thus, care was taken to excite the sample with as low intensity as possible, but with enough intensity to give a reasonable signal-to-noise ratio. In Figure 4, typical transient absorption traces after B800 excitation are shown, together with exponential fits. The traces indicate that annihilation effects are very small (additional negative signals are not present and ESA can be seen). Ground-state bleaching at 800 nm, immediately after excitation (a), arrival of excitation from B800 to B850, excited-state absorption below 840 nm (b), and ground-state

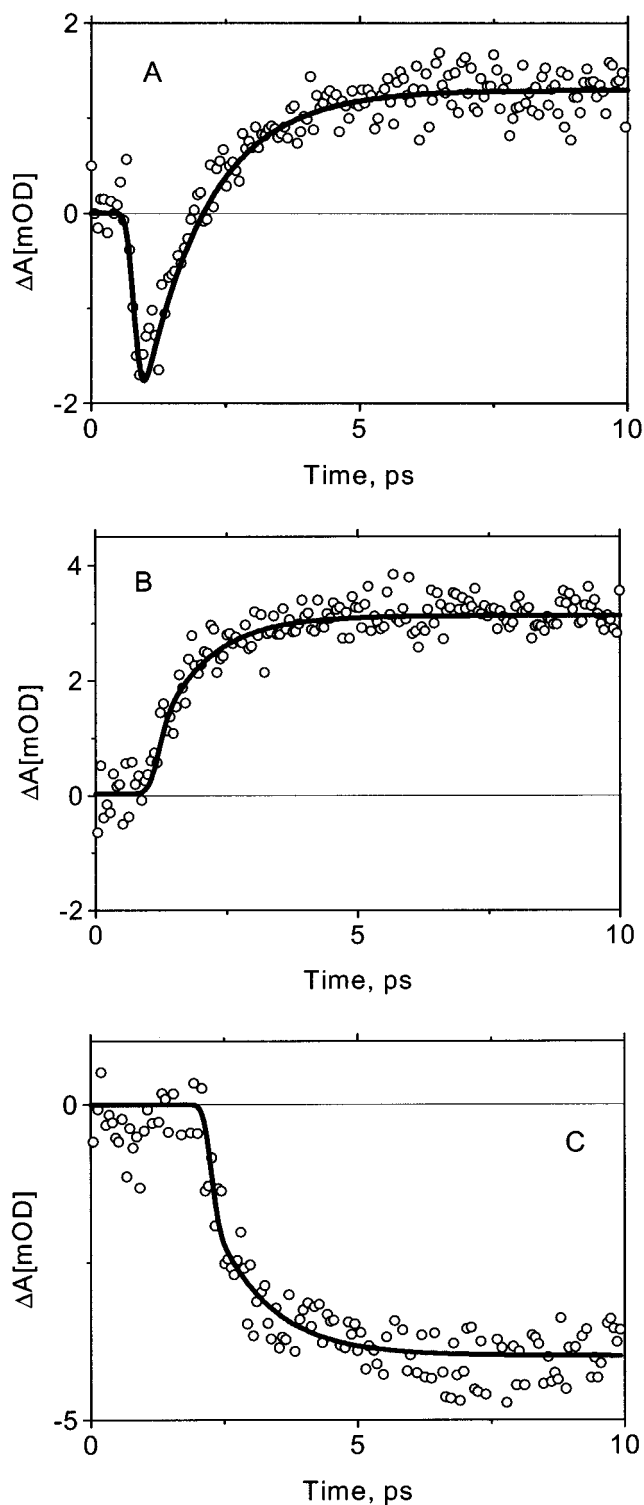


Figure 4. Typical room-temperature transient absorption traces together with kinetic fits after B800 excitation and detection at 810 nm (A), at 830 nm (B), and at 850 nm (C).

bleaching around 850 nm plus stimulated emission in the red edge of the detection wavelength (c) are shown in Figure 4. The transient absorption data were fitted globally with a sequential model containing two components (See Materials and Methods). The lifetimes assigned to energy transfer from B800 to B850 varied between 0.5 and 1.2 ps (Table 1), depending on the excitation wavelength around 800 nm. Although the differences in EET rates are small (790 nm vs 810 nm) the main trend was that excitation at 800 nm always induces a faster energy transfer time (0.9 ps) than excitation at either 790 or

TABLE 1: Lifetimes at Several Excitation Wavelength Corresponding Excitation Energy Transfer (EET) from B800 to B850^a

pump wavelength, nm	τ_{EET} (B800 \rightarrow B850), ps	
	exp	calc
790	1.2	1.3
800	0.9	0.8
810	1.0	0.9
830	0.5	0.4

^a The experimental transfer times from B800 to B850 are in the left and the calculated in the right column. In the calculations, all transitions from the energy levels excited by the pump pulse to the B850 band were included.

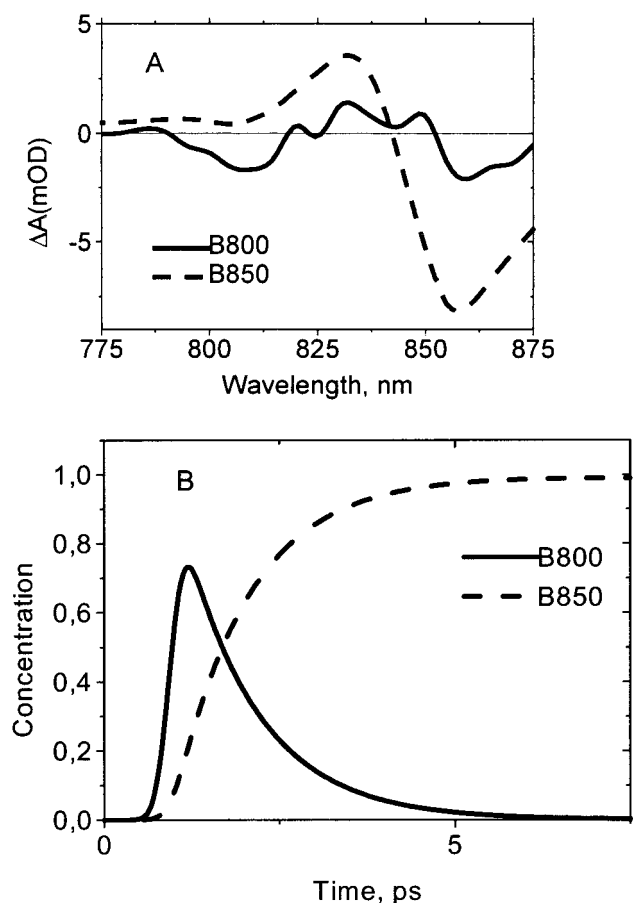


Figure 5. Transient absorption difference spectra of LH2 antenna at room temperature with 810 nm excitation, analyzed with a sequential model with two components. Species associated difference spectra (A) and concentration profiles (B). The solid line corresponds to the B800 states with a decay lifetime of 1.0 ps (Table 1) and the dashed line represents formation of the long-lived B850 state.

810 nm. The trend was seen on each experimental set of data, and the effect is reproducible given the signal-to-noise ratio of the experiment. With excitation at 830 nm, the fastest time constant (0.5 ps) was observed. A long lifetime component (>200 ps) was added in the fittings, representing the lifetime of B850 (k_2 in the fitting model). This time constant was not accurately determined because the time window of the experiment was only 15 ps. A lifetime of 1 ns of B850 of the isolated LH2 complex has been determined experimentally.³⁹ The SADS (A) and concentration profiles (B) according to the fitting model are shown in Figure 5. The solid decaying concentration profile represents the disappearance of population of the excited state of the B800 states, whereas the dashed rising component represents the growth of population of the excited state of the

B850 system. The B800 spectrum resembles a bleaching band around 800 nm and is very similar to that obtained by Kennis et al.²⁰ Slight excited-state absorption around 830 nm and bleaching below 850 nm can be seen, which may reflect early time energy transfer to the B850 band. Because low excitation energy is used, the bleaching signal at 800 nm is not very strong and errors in baseline corrections and in estimation of time zero may contribute to the spectrum. Accordingly, the interpretation of the spectral behavior on the red side of the B800 band has to be taken as tentative only. After energy transfer the B850 SADS predominates (dashed curve), bleaching around 850 nm is clearly visible. The ESA starts from 770 nm and is visible up to 840 nm. It may continue toward longer wavelengths although it is difficult to resolve because of the overlap of bleaching and stimulated emission in this region. The shape of the B850 SADS spectrum turned out to be independent of the excitation wavelength used. Similar B850 spectra have been obtained for LH2 B800–850 complexes from other species.⁶

The calculated B800–B850 energy transfer times are shown in the right column of Table 1. The absolute values of the calculated time constants agree very well with those obtained from the experiments. Especially, the same trend as in the experiments is clearly visible, excitation at 800 nm induces faster energy transfer to B850 as compared to excitations at 790 and 810 nm. This is to be expected as there is best overlap of the B850 excitonic states (E_3 states) with B800 states at 800 nm (see Figure 3). With excitation at 830 nm the fastest energy transfer rate of 0.4 ps is obtained. To explain this, we want to draw attention also to the $1,2E_2$ states, located around 824 nm (see Figure 3). These states have only very small oscillator strengths (about 10 000 times smaller than that of the E_1 state of B850), and they are therefore not seen in the steady-state absorption spectrum. However, for energy transfer from B800 to B850, according to our model, they play an important role. When 830 nm excitation is used, the overlap of the $1,2E_2$ states with excited B800 states and with the E_1 states of B850 provides a natural route for the very fast 0.5 ps energy transfer to B850 at this excitation.

To study B800, intra-ring energy transfer polarized transient absorption measurements were performed. Induced polarization may decay due to energy transfer between similar chromophores of the B800 ring, EET from B800 to B850 and ESA (in this case below 815 nm; see Figure 4) as the transition dipole orientation may be different for the ESA than for the ground-state absorption. To distinguish between the different processes, the anisotropy values for the bleaching and for the ESA were estimated from the measured anisotropy data. The anisotropy decay kinetics was then analyzed according to the well-known relations between polarized absorption and isotropic absorption:

$$\Delta A(\parallel) = \Delta A(\text{iso})[1 + 2r(t)] \quad (1a)$$

$$\Delta A(\perp) = \Delta A(\text{iso})[1 - r(t)] \quad (1b)$$

An associative model¹² was used. For each component an anisotropy that was either time independent or exponentially decaying was tried. It turned out that the data were well fitted with a time independent anisotropy and that the parameters of an exponentially decaying anisotropy could not precisely be estimated with the present signal-to-noise ratio.

In Figure 6 the decay curves of the polarized measurements after 810 nm excitation are shown at three different probe polarizations, parallel, magic angle, and perpendicular. The fitted decay traces (present in the figure as dashed lines) follow the experimental curves very closely. The estimated anisotropy

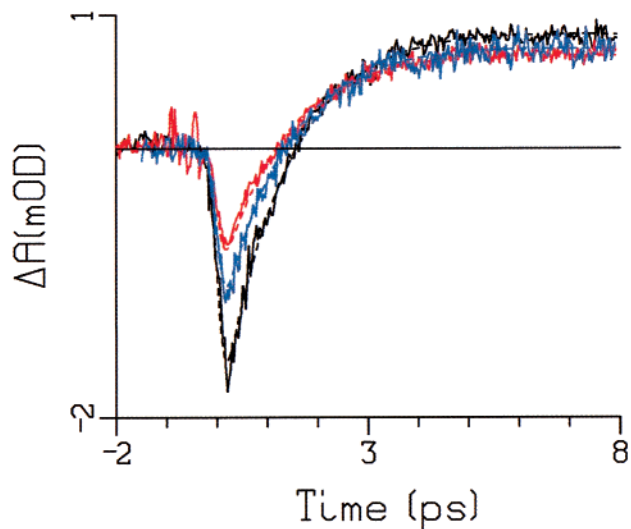


Figure 6. Typical transient absorption traces (solid lines) probed with parallel (black), magic angle (blue), and perpendicular (red) polarization with respect to the excitation light. The dashed lines are fits of the anisotropy traces according to the eq 1 and values of Table 2. The excitation and detection wavelength was 810 nm.

TABLE 2: Estimated Initial and Final Anisotropy Values (Second Column) and Calculated Excitation Energy Transfer Times of Averaged Single Transfer between B800 States (Third Column)

pump wavelength, nm	$r_0; r_{inf}$ (exp)	$\tau_{\text{single step EET (B800) (calc), ps}$
790	0.17; 0.08	0.1 and 0.6
800	0.42; 0.26	0.1
810	0.25; 0.07	0.1
830		0.9

parameters are shown in Table 2. With 790 and 810 nm excitations the initial anisotropy values were 0.17 and 0.25, respectively. The calculated times of an averaged *single* energy transfer step between excitonic B800 states in the spectral range from 790 to 810 nm, with 790, 800, and 810 nm excitation pulses, respectively, are also shown in Table 2 (third column). The calculated energy transfer time at 790 nm excitation from the blue side to the red side of the B800 band was about 100 and 600 fs, whereas with 800 and 810 nm excitations the single step intra-ring energy transfer takes place very fast, in about 100 fs. Comparison of the experimentally determined initial anisotropy values and calculated averaged single excitation transfer times suggests that the excitation motion within the B800 band is fast as compared to EET from B800 to B850. This would explain the low initial anisotropy values obtained at 790 and 810 nm. With the present time resolution it would have been impossible to resolve this fast component. The situation at the center of the absorption peak at 800 nm is somewhat strange since the initial anisotropy obtained was 0.4, suggesting that no intra B800 ring transfer had taken place during the excitation. Presently, we do not have a good explanation for this and do not exclude a possibility for experimental uncertainty at this wavelength. The overall description given on intra-ring B800 transfer is somewhat different from that of Salverda et al., where excitation movements were studied by a three-pulse photon echo experiment, and a single hopping time of 1.6 ps between the B800 pigments was reported.¹⁸

Discussion

According to biochemical studies, the homology of the LH2 antenna of *Rs. molischianum* with the LH1 antenna complexes

of purple bacteria, is higher than that with LH2 complexes from other species.⁴⁰ Resonance Raman studies suggests that the two main amino acids, which are involved in hydrogen-bonding to the BChl *a*, are the two tryptophans α -Trp 45 and β -Trp44. They are clearly within H-bonding distance from the 2-acetyl carbonyl oxygen atoms of the B850 BChl *a* molecules.^{3,40} Moreover, the orientation of the B800 pigments is different in *Rs. molischianum* as compared to *Rps. acidophila*. The ligating amino acid in *Rs. molischianum* B800 is aspartate whereas in *Rps. acidophila* B800 it is formylmethionine.³ Our calculations showed that only after inclusion of these and several other amino acids in estimation of site energies of BChl *a* molecules in the protein and using these in excitonic calculations could the absorption and CD spectrum be successfully simulated. Recently, by using the above-mentioned semiempirical method (ZINDO/S CIS), absorption spectra of known Chl's and BChl's in various solvents could be successfully simulated.^{41,42} The results clearly demonstrate solvent perturbation of the excited-state energies of the chromophores in solution. Similar interactions are functional for monomeric pigments in the protein environment. Our calculated site energies of BChl *a* molecules of the B800 ring, where excitonic interactions are known to be small and which are far too small to explain the experimentally observed spectral shifts, are in very nice agreement with the experimental values for both *Rps. acidophila*³⁰ and *Rs. molischianum*. After obtaining excitonic energy levels that describe the absorption and CD spectra correctly, the energy transfer rates from B800 to B850 were calculated as well.

We want to point out that there are a number of studies where absorption or CD spectrum or energy transfer rates between B800 and B850 with different sets of parameters have been reported. As far as we know there are no studies that have been able to simulate both experimental steady-state absorption and CD spectra and energy transfer rates with a single set of a few experimental input parameters. By using the CIEM method, it has been possible to accomplish this. The method can be applied to any aggregated chromophore system in any environment for which the atomic structure is known. One fundamental question that concerns theoretical predictions is the reliability of estimation of site energies of pigments in the protein environment. In many studies site energies of the B850 pigments have been put, without detailed investigations, in the range from 800 to 830 nm and used for the excitonic calculations.^{6,37,43,44} Our approach avoids such uncertainties, the site energies are calculated in a systematic manner by using computational methods that rely on atomic coordinates of the system and are only slightly dependent on the quantum chemical method used. Some theoretical calculations have been done for the LH2 complex for one species and the results are compared to experimental values from another species.^{6,25,45} In light of the results obtained for *Rps. acidophila*³⁰ and *Rs. molischianum* in the present paper, such comparison seems dubious.

According to our calculations the excitonic states that are mostly responsible for the energy transfer from B800 to B850 are the 3,4E₁ states of the B800 ring and the 1,2E₃ and 1,2E₂ states of the B850 ring. This interpretation is based on the fact that faster B800–B850 energy transfer is observed, both experimentally and theoretically, with 800 nm excitation and slower rates for both 790 and 810 nm excitations. Although the experimental values do show only small differences, the trend in the calculated energy transfer rates is doubtless the same (see Table 1). Moreover, the observed very fast energy transfer rate of 0.5 ps, when 830 nm excitation is used, suggests that also the “dark” 1,2E₂ states (located at 824 nm with small

oscillator strength) are involved in energy transfer to B850. From calculated excitonic manifolds we can see that in the LH2 of *Rs. molischianum* the E_2 state is the only state between 800 and 850 nm (see Figure 3), whereas in *Rps. acidophila* two dark states ($1,2E_3$ and $1,2E_2$) are present.³⁰ As energy gaps are smaller in LH2 of *Rps. acidophila* than in LH2 of *Rs. molischianum*, faster energy transfer may occur in the former, in accord with the experimental findings. Our results are also a manifestation of dependence of the observed kinetic constants on preparation of the initial state and probing of the final states. Experimental kinetic results are dependent on energy and intensity distributions (pulse shape) of the excitation and probe pulses and their overlap with the excited-state energy levels of the sample under study.

We could not resolve any subpicosecond (250–600 fs) component with excitation wavelengths between 790 and 810 nm, neither in the isotropic decay analysis nor in the anisotropy analysis. Calculations predicted a fast (~100 fs) energy transfer component between the B800 states at each excitation wavelength used. With 790 nm excitation an additional calculated 600 fs component for intra B800 band energy transfer was obtained. In many energy transfer studies of LH2 complexes a component of about 400 fs has been observed and assigned to intra-ring energy equilibration (see Introduction). On the basis of our experimental findings and theoretical results, we suggest that intra B800 ring energy transfer in LH2 of *Rs. molischianum* takes place much faster than in LH2 of *Rbs. acidophila*, faster than our instrument response (~250 fs). After equilibration, B800 to B850 energy transfer takes place at equal probability from the weakly coupled excitonic states of the B800 ring. As mentioned before, this is quite a different picture from that of Joo et al. and Salverda et al., who have suggested that the B800–B800 energy transfer/vibrational relaxation in LH2 of *Rs. molischianum* at low temperatures takes place within 0.7–1.1 ps.^{15,18}

Conclusions

In this article we have presented both experimentally determined and calculated absorption and CD spectra and energy transfer rates of the LH2 complex from *Rs. molischianum*. By using a fully excitonic model, the CD spectrum of this complex has been simulated for the first time. The transition and interaction energies of the pigments were calculated by using a scaled semiempirical quantum chemical CI method, and the nearby amino acid environment of the pigments was included in the calculations. The experimental value of the transition moment of Bchl *a*, homogeneous and inhomogeneous line widths and the mean dielectric constant of the protein were the other input parameters in the calculations. Statistical variation of the elements of the exciton matrix was used to account for disorder.

The room-temperature B800–B850 energy transfer times of ~1.0 ps were observed with excitation wavelengths around 800 nm. The time is longer than the corresponding rate in *Rps. acidophila* and in *Rb. sphaeroides*. Slight variations (0.9–1.2 ps) in B800–850 energy transfer times were found with excitation wavelengths between 790 and 810 nm, 0.9 ps transfer occurring at 800 nm excitation. At 830 nm excitation the energy transfer to the B850 ring takes place within 0.5 ps. The same parameter set that produced the absorption and CD spectra correctly was used to calculate energy transfer rates by using Fermi's Golden rule. In the calculations the experimental spectral widths of excitation and probe pulses used were used to "create" the initial excited state and to "probe" the final states.

The calculated energy transfer rates fitted nicely with the experimental results and suggest that the B850 states $3,4E_3$ at 798 nm and $1,2E_2$ at 824 nm serve as effective channels in the B800–B850 energy transfer in LH2 of *Rs. Molischianum*.

Acknowledgment. We acknowledge the financial support from the University of Jyväskylä (scholarship for J.I.) and from the Academy of Finland (J.L., contracts 34192 and 44546; J.K. and P.M. the MATRA program, contract 40416). M.Sc. Jani Kallioinen is acknowledged for technical assistance and discussions.

References and Notes

- (1) Blankenship, R. E.; Madigan, M. T.; Bauer, C. E. *Anoxygenic Photosynthetic Bacteria*; Kluwer Academic Publishers: Dordrecht, The Netherlands, 1995.
- (2) van Grondelle, R.; Dekker, J. P.; Gillbro, T.; Sundström, V. *Biochim. Biophys. Acta* **1995**, *1187*, 1.
- (3) Koepke, J.; Hu, X.; Muenke, C.; Schulten, K.; Michel, H. *Structure* **1996**, *4*, 581.
- (4) McDermott, G.; Prince, S. M.; Freer, A. A.; Hawthornthwaite-Lawless, A. M.; Papiz, A. M.; Cogdell, R. J.; Isaacs, N. W. *Nature* **1996**, *374*, 517.
- (5) Visschers, R. W.; Germeroth, L.; Michel, H.; Monshouwer, R.; van Grondelle, R. *Biochim. Biophys. Acta* **1995**, *1230*, 147.
- (6) Sundström, V.; Pullerits, T.; van Grondelle, R. *J. Phys. Chem. B* **1999**, *103*, 2327.
- (7) Leupold, D.; Stiel, H.; Ehlert, J.; Nowak, F.; Teuchner; Voigt, B.; Bandilla, M.; Ücker, B.; Scheer, H. *Chem. Phys. Lett.* **1999**, *301*, 537.
- (8) Leupold, D.; Voigt, B.; Benken, W.; Stiel, H. *FEBS Lett.* **2000**, *480*, 73.
- (9) Oijen, A. M.; Ketelaars, M.; Köhler, J.; Aartsma, T. J.; Schmidt, J. *Science* **1999**, *285*, 400.
- (10) Monshouwer, R.; de Zarate, I. O.; van Mourik, F.; van Grondelle, R. *Chem. Phys. Lett.* **1995**, *246*, 341.
- (11) Pullerits, T.; Hess, S.; Herek, J. L.; Sundström, V. *J. Phys. Chem. B* **1997**, *101*, 10560.
- (12) Wendling, M.; van Mourik, F.; van Stokkum, I. H. M.; Salverda, J. M.; Michel, H.; van Grondelle, R. In *Photosynthesis: Mechanisms and Effects*; Garab, G., Ed.; Kluwer Academic Publishers: Dordrecht, The Netherlands, 1998; Vol. I, p 49.
- (13) De Caro, C.; Visschers, R. W.; van Grondelle, R.; Völker, S. *J. Phys. Chem.* **1994**, *98*, 10584.
- (14) Hess, S.; Feldchtein, F.; Babin, A.; Nurgaleev, I.; Pullerits, T.; Sergeev, A.; Sundström, V. *Chem. Phys. Lett.* **1993**, *216*, 247.
- (15) Joo, T.; Jia, Y.; Yu, J.-Y.; Jonas, D. M.; Fleming, G. R. *J. Phys. Chem. B* **1996**, *100*, 2399.
- (16) Ma, Y.-Z.; Cogdell, R. J.; Gillbro, T. *J. Phys. Chem. B* **1997**, *101*, 1087.
- (17) Ma, Y.-Z.; Cogdell, R. J.; Gillbro, T. *J. Phys. Chem. B* **1998**, *102*, 881.
- (18) Salverda, J. M.; van Mourik, F.; van der Zwan, G.; van Grondelle, R. *J. Phys. Chem. B* **2000**, *104*, 11395.
- (19) Lin, S. H.; Alden, R. G.; Hayashi, M.; Suzuki, S.; Murchison, H. A. *J. Phys. Chem.* **1993**, *97*, 12566.
- (20) Kennis, J. T. M.; Streltsov, A. M.; Vulto, S. I. E.; Aartsma, T. J.; Nozawa, T.; Amesz, J. *J. Phys. Chem. B* **1997**, *101*, 7827.
- (21) Wu, H. M.; Reddy, N. R. S.; Cogdell, R. J.; Muenke, C.; Michel, H.; Small, G. J. *Mol. Cryst. Liq. Cryst.* **1996**, *291*, 163.
- (22) Fraser, N. J.; Dominy, P. J.; Ücker, B.; Simonin, I.; Scheer, H.; Cogdell, R. J. *Biochemistry* **1999**, *38*, 9684.
- (23) Herek, J. L.; Fraser, N. J.; Pullerits, T.; Martinsson, P.; Polivka, T.; Scheer, H.; Cogdell, R. J.; Sundström, V. *Biophys. J.* **2000**, *78*, 2590.
- (24) Förster, T. *Ann. Phys.* **1948**, *6*, 55.
- (25) Scholes, G. D.; Fleming, G. R. *J. Phys. Chem. B* **2000**, *104*, 7275.
- (26) Kruger, B. P.; Scholes, G. D.; Gould, I. R.; Fleming, G. R. *PhysChemComm.* **1999**, *8*.
- (27) Sumi, H. *J. Phys. Chem. B* **1999**, *103*, 252.
- (28) Linnanto, J.; Korppi-Tommola, J. E. I. *J. Chin. Chem. Soc.* **2000**, *47*, 657.
- (29) Mukai, K.; Abe, S.; Sumi, H. *J. Luminescence* **2000**, *87–89*, 818.
- (30) Linnanto, J.; Korppi-Tommola, J. E. I.; Helenius, V. M. *J. Phys. Chem. B* **1999**, *103*, 8739.
- (31) van Stokkum, I. H. M.; Scherer, T.; Brouwer, A. M.; Verhoeven, J. W. *J. Phys. Chem.* **1994**, *98*, 852.
- (32) Cory, G. C.; Zerner, M. C.; Hu, X.; Schulten, K. *J. Phys. Chem. B* **1998**, *102*, 7640.

- (33) Hu, X.; Damjanovic, A.; Ritz, T.; Schulten, K. *Proc. Natl. Acad. Sci. U.S.A.* **1998**, *95*, 5935.
- (34) Tretiak, S.; Middleton, C.; Chernyak, V.; Mukamel, S. *J. Phys. Chem. B* **2000**, *104*, 4519.
- (35) Tretiak, S.; Middleton, C.; Chernyak, V.; Mukamel, S. *J. Phys. Chem. B* **2000**, *104*, 9540.
- (36) Linnanto, J.; Ihalainen, J. A.; Korppi-Tommola, J. E. I. Manuscript in preparation.
- (37) Koolhaas, M. H. C.; Frese, R. N.; Fowler, G. J. S.; Bibby, T. S.; Georgakopoulou, S.; van der Zwan, G.; Hunter, C. N.; van Grondelle, R. *Biochemistry* **1998**, *37*, 4693.
- (38) Bandilla, M.; Ücker, B.; Ram, M.; Simonin, I.; Gelhaye, E.; McDermott, G.; Cogdell, R.; Scheer, H. *Biochim. Biophys. Acta* **1998**, *1364*, 390.
- (39) Freiberg, A.; Jackson, J. A.; Lin, S.; Woodbury, N. W. *J. Phys. Chem. A* **1998**, *102*, 4372.
- (40) Germeroth, L.; Lottspeich, F.; Robert, B.; Michel, H. *Biochemistry* **1993**, *32*, 5616.
- (41) Linnanto, J.; Korppi-Tommola, J. E. I. *Phys. Chem. Chem. Phys.* **2000**, *2*, 4962.
- (42) Linnanto, J.; Korppi-Tommola, J. E. I. *J. Phys. Chem. A* **2001**, *106*, 3855.
- (43) Pullerits, T.; Chachivilis, M.; Sundström, V. *J. Phys. Chem.* **1996**, *100*, 10787.
- (44) Koolhaas, M. H. C.; van der Zwan, G.; van Grondelle, R. *J. Phys. Chem. B* **2000**, *104*, 4489.
- (45) van der Zwan, G. Personal communications.